RSC Advances

PAPER

View Article Online
View Journal | View Issue

Cite this: *RSC Adv.*, 2018, **8**, 40321

Adsorption behavior and mechanism of β-cyclodextrin–styrene-based polymer for cationic dyes

Xia Li, * Long Xie, Xuan Yang and Xiaojuan Nie

Cyclodextrin polymers are efficient adsorbents for dye adsorption. Herein, a β-cyclodextrin polymer (β-CDSP) with carboxyl groups and benzene rings was prepared *via* free radical polymerization of β-cyclodextrin-maleate and styrene. The adsorption performance of β-CDSP was studied by adsorbing neutral red (NR), basic fuchsin (BF) and safranine T (ST) dyes under different adsorption conditions (*e.g.*, adsorption time, temperature and pH of the solution). The results showed that the adsorption of BF and ST was faster and better than that of NR. The adsorption kinetic behavior fitted well with both the pseudo-first-order and the pseudo-second-order models for NR and BF, but it fitted better with the latter for ST. The adsorption equilibrium data followed the Langmuir isotherm model. The adsorption process was endothermic and spontaneous, and a higher temperature was favorable for dye adsorption. Higher q_t values were obtained in a basic medium, which resulted from the electrostatic interactions between β-CDSP and cationic dyes. Furthermore, inclusion complexion and π–π interactions also contributed to the dye adsorption. The stability and reusability of β-CDSP were estimated by four regeneration cycles.

Received 17th September 2018
Accepted 17th November 2018

DOI: 10.1039/c8ra07709f

rsc.li/rsc-advances

Introduction

Dyes, as a relatively large group of organic compounds with complicated structures, find extensive utility in textile, leather, printing, paper, rubber, plastic, pharmaceutical and food industries to color their products.[1–3] Meanwhile, wastewater caused by dyes is a serious threat to the environment and human safety due to the toxic effects and because degradation of dyes is difficult. Many studies have raised great concerns about the research on the adsorption of dyes by different adsorbents.

Cyclodextrins (CDs) are a series of cyclic oligosaccharides consisting of six (α-CDs), seven (β-CDs) or eight (γ-CDs) anhydrous D-glucopyranose units (AGU) bonded through α-(1,4) glycosidic linkages. CDs have attracted great attention owing to their specific chemical structures with truncated cone cavities since they were discovered by Villiers. The hydrophobic internal surface of a CD cavity is formed by glycosidic oxygens and methane protons, which can form inclusion complexes with many organic molecules through non-covalent interactions.[4–6] The hydroxyl groups located on the rim of the cavity make the external surface of the cavity hydrophilic. Importantly, the hydroxyl groups can be substituted by different organic groups to form various CD derivatives, which have been widely used in the fields of pharmaceutics, separation, food, life and environment science.[7–11] Especially for the treatment of wastewater, adsorption using cyclodextrin-based polymers (CDPs) as adsorbents is an efficient technique because of its specific affinity, simple operation and low cost.[12]

CDPs are often prepared by the reaction of cyclodextrins with crosslinking reagents or by grafting cyclodextrins on other polymers. Grégorio Crini *et al.* used CDPs containing carboxylic groups and hydroxyl groups for the removal of C. I. Basic Blue 9 and cationic dyes (C. I. Basic Blue 3, Basic Violet 3 and Basic Violet 10), respectively.[13,14] High adsorption capacity of the adsorbent was exhibited toward these dyes. Elif Yilmaz *et al.* prepared CDPs using 4,4′-methylene-bisphenyl diisocyanate or hexamethylene diisocyanate as a cross linking agent, and they used them for adsorbing azo dyes (Evans Blue and Chicago Sky Blue) and aromatic amines.[15] The results indicated that physical adsorption, hydrogen bonding interactions and the formation of an inclusion complex between the host and guest play important roles in the adsorption. Furthermore, cross-linked chitosan/β-cyclodextrin composites[16,17] and cyclodextrin-based nano-adsorbents[18–20] were also widely developed and utilized in the adsorption for many types of dyes because of their specific adsorption capacity.

In this paper, a novel water-insoluble β-cyclodextrin–styrene-based polymer (β-CDSP) was synthesized successfully by the copolymerization of β-cyclodextrin-maleate and styrene. Three cationic dyes with conjugate aromatic rings and amino groups, *i.e.*, neutral red (NR), basic fuchsin (BF) and safranine T (ST), which have wide applications in industries,[21,22] were

The Department of Chemistry, School of Science, North University of China, Shanxi 030051, PR China. E-mail: lixia200688@126.com

determined as adsorbates to evaluate the adsorption performance of β-CDSP. Several important parameters affecting the adsorption capacity (*e.g.*, adsorption time, temperature and pH of the solution) were studied and analyzed during the three dye adsorption process and the possible mechanism was discussed. Furthermore, the reusability of β-CDSP was evaluated *via* sequential adsorption–desorption cycles.

Experimental

Materials

β-Cyclodextrin was obtained from the Kermel Chemical Reagent Factory of Tianjin (Tianjin, China). Maleic anhydride (MA), sodium hydride (60%), *N*,*N*-dimethylformamide (DMF) and styrene were purchased from Tianjin Chemical Reagent Factory No. 3 (Tianjin, China). DMF was dried and redistilled before use. Dibenzoyl peroxide (BPO) was purchased from Nanjing Chemical Reagent Factory (Nanjing, China). The three dyes NR, BF and ST (please see Scheme 1 for their structural formulas) were supplied by Sinopharm Chemical Reagent Co. Ltd (Shanghai, China). All the chemicals and reagents used were of analytical grade.

Preparation of β-CDM

β-CD (2.27 g, 2 mmol) was completely dissolved in dry DMF (40 mL), and solid sodium hydride (0.48 g, 12 mmol) was slowly added with vigorous stirring. After being magnetically stirred at room temperature for 24 h, solid MA (1.372 g, 14 mmol) was slowly added into the solution. The mixture was stirred for an additional 48 h at room temperature and then added drop-wise into acetone. A white product was precipitated and washed with acetone 3–5 times. After being dried in vacuum at room temperature, the obtained β-CDM was kept in a sealed glass vacuum desiccator.

Preparation of β-CDSP

The copolymerization of β-CDM and styrene was performed by the following procedure. First, β-CDM (1.2 g) and styrene (3.1 g) were dissolved in benzene (25 mL) under constant stirring. Second, the initiator of BPO (0.04 g) was slowly added into the solution. Then, the mixture was heated to 80 °C and stirred for another 4 h at this temperature. The reaction product was precipitated with methanol and then washed with a large quantity of distilled water 3–5 times to remove unreacted β-CDM. Thereafter, the obtained white solid products were washed with methanol again and dried in a vacuum desiccator at 50 °C for 8 h.

Characterization and stability of β-CDSP

The FTIR spectra of β-CDM and β-CDSP were measured using the KBr disc method on a Bruker VERTEX 70 instrument. The mixed powder was compressed into a transparent disk and scanned from 4000 to 400 cm^{-1} using an average of 16 scans with a resolution of 1 cm^{-1}. The ^{1}H NMR and ^{13}C NMR spectra were recorded on a Bruker Avance 600 spectrometer at 600 MHz. β-CDSP was dissolved in $CDCl_3$ as the solvent. Scanning electron microscopy (SEM) of the sample was conducted using FEI Inspect F50. X-ray diffraction patterns (XRD) of β-CD and β-CDSP were acquired from 5 to 85°on a Bruker D8 ADVANCE A25X instrument. The molecular weight (M_w) of β-CDSP was measured by gel permeation chromatography (GPC) on an Agilent PLGPC220 instrument using *N*,*N*-dimethylformamide as a solvent. To investigate the thermal stability and degradation behavior of β-CDSP, the TGA curves of β-CD and β-CDSP were measured on a Mettler Toledo TGA1 instrument under nitrogen flow. The weight loss of β-CD and β-CDSP was monitored from 0 to 800 °C at a rate of 10 °C min^{-1}.

Adsorption experiments

In this study, batch adsorption experiments were performed by the following method: 50 mg adsorbent was mixed with 50 mL dye aqueous solution with a certain concentration in a 150 mL closed conical flask. Stock solutions of the three dyes (50 mg L^{-1}) were prepared in double-distilled water. The desired experimental solutions of dyes were obtained by successive dilution of these stock solutions with double-distilled water. The adsorption of NR, BF and ST on β-CDSP was studied at different adsorption times (30–180 min), pH values (2–12) and temperatures (298–338 K). All the experiments were performed at a constant shaking rate of 300 rpm. The temperature of adsorption was determined by a temperature-controlled shaking water bath. The pH value of the aqueous solution, monitored with a pH meter, was adjusted by adding 0.01 M HCl or 0.01 M NaOH. After stirring for a certain time, the adsorbent was removed by centrifugation before measurements, and the corresponding supernatant was analyzed by a TU-1800 UV-vis spectrophotometer at 523 nm for NR, 544 nm for BF and 554 nm for ST. The calibration curves of the dyes

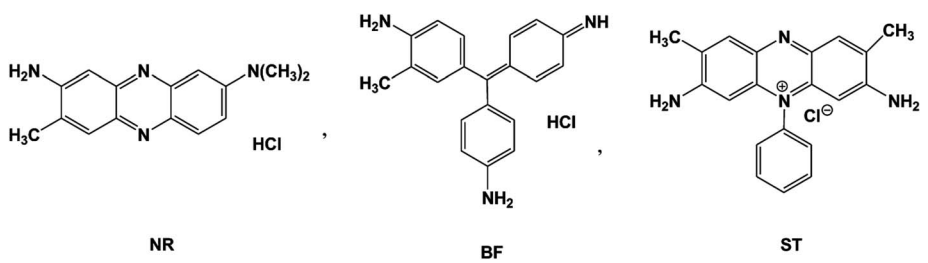

Scheme 1 Chemical structures of dyes.

were first obtained and used to convert absorbance data into concentrations during the adsorption experiments.

The amount of each dye absorbed by β-CDSP, *i.e.*, q_t was calculated with the following formula:

$$q_t = \frac{V(C_0 - C_t)}{W}$$

Here, q_t (mg g^{-1}) is the adsorption capacity at real time t, V (L) is the volume of dye in the aqueous solution, C_0 (mg L^{-1}) and C_t (mg L^{-1}) are the initial and real-time concentrations of dye solution, respectively, and W (g) is the weight of β-CDSP.

Results and discussion

Characteristics of β-CDSP

The FTIR spectra of β-CDSP together with that of β-CDM as a comparison are shown in Fig. 1a. The peaks at around 3384, 2848 and 2922 cm^{-1} were assigned to O–H and C–O stretching vibrations for C-2 and C-3 from cyclodextrin in the β-CDSP spectrum. The peaks at 1720 and 1662 cm^{-1} observed in the β-CDM spectrum were assigned to C=O and C=C stretching vibrations from dienoic acid ester groups. After copolymerization with styrene, the peak at 1662 cm^{-1} disappeared in the β-CDSP spectrum. The new peaks from 3026 to 3064 cm^{-1} originated from C–H stretching vibrations, and the peaks at 1581, 1491, 1452, 760 and 696 cm^{-1} corresponded to C–H bending vibrations of benzene rings from a cyclodextrin–styrene-based polymer. These results suggested that β-CDSP has been successfully synthesized.

Fig. 1b shows the ^{1}H NMR spectrum of β-CDSP. The peaks at 0.77–2.18 ppm were ascribed to the protons of –OH, $–CH_2–$ and –CH– on CDs and alkyl chains, and the peaks at 6.34–7.31 ppm were identified as the protons of –CH– in benzene rings. The ratio of the integrated peak areas of a ~ l and m ~ o was 1 : 1.23. For the ^{13}C NMR spectrum (Fig. 1c), the peaks (e, i ~ l) at 28.69 ppm and 39.37–43.16 ppm were assigned to carbons of alkyl chains. The peaks (b ~ d, f) at 75.79 and 76 ppm were

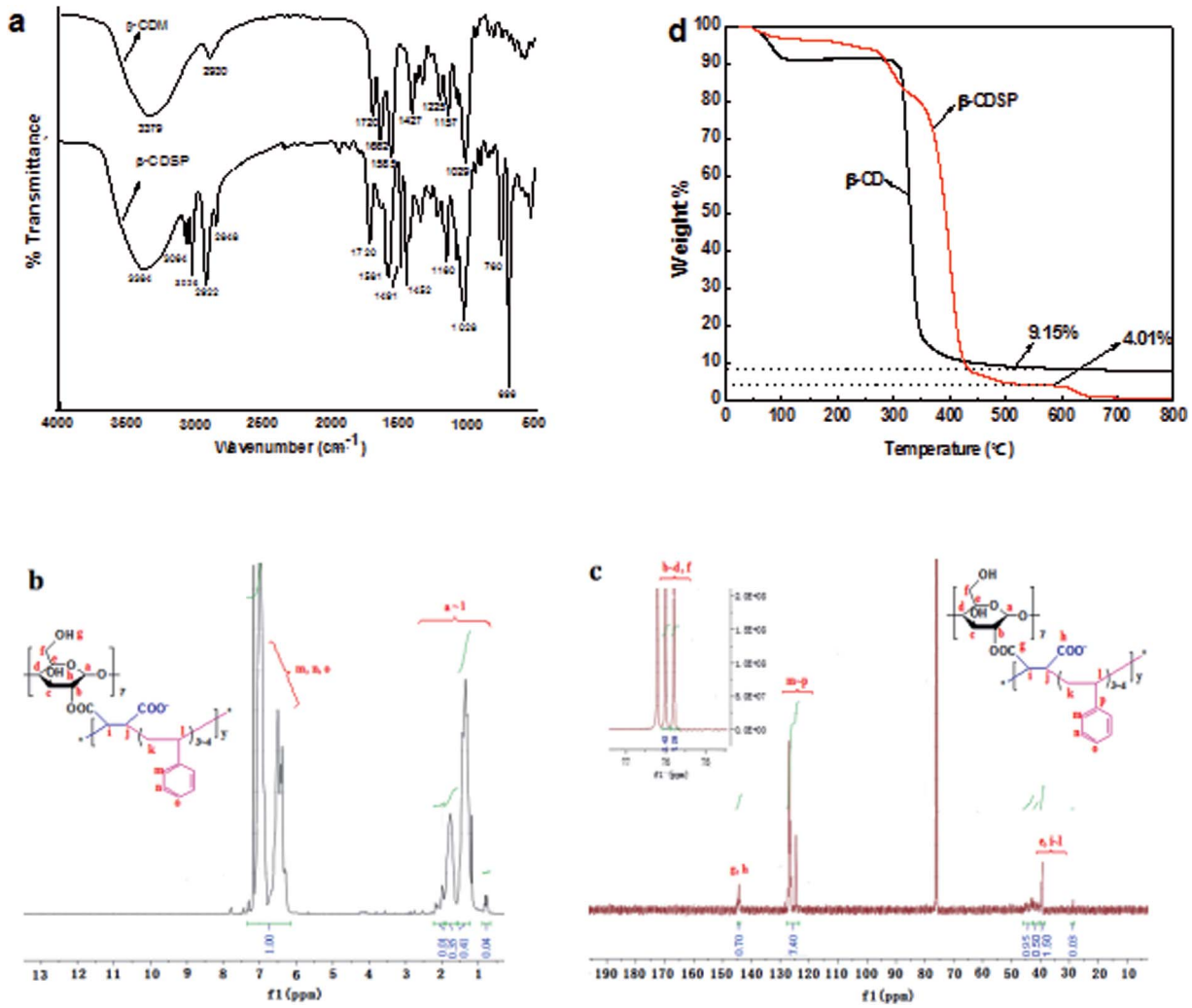

Fig. 1 (a) FTIR spectra of β-CDSP and β-CDM; (b) ^{1}H NMR spectrum of β-CDSP; (c) ^{13}C NMR spectrum of β-CDSP; (d) TGA curves of β-CD and β-CDSP.

ascribed to the carbons from C–O of the polymer, whereas the signals of carbons from ester groups (g, h) were found at 144.19 and 144.30 ppm. Moreover, the peaks (m ∼ p) at 124.46–128.47 ppm corresponded to the carbons of C=C of benzene rings. The ratio of the integrated peak areas of g, h and m ∼ p was 1 : 10.55. These data verified the successful polymerization of β-CDM and styrene.

Fig. 2a shows the powder X-ray diffraction pattern of β-CDSP, where the result for β-CD is presented for comparison. It is clear that the crystalline feature of β-CD decreased after polymerization with styrene because of the formation of new covalent bonds of β-CDSP. The new broader diffraction angles (2θ) at 10.9° and 19.1° observed for β-CDSP were assigned to the amorphous structure of the polymer, which resulted from phenethyl groups that increased the randomness of the amorphous region.[23] The surface morphology of β-CDSP was characterized with SEM, as shown in Fig. 2b. It can be seen that β-CDSP exhibited a granular and porous structure with mostly irregular shapes because of the formation of covalent bonds between β-CDM and styrene.[24] The porous structure was beneficial for the access of the dye molecules into the interior of β-CDSP, which may result in good adsorption of dyes. The molecular weight of β-CDSP was measured by GPC, and the value of M_w was 451 056.

The thermal stability and degradation behavior of β-CDSP were evaluated by TGA (Fig. 1d). In the first stage, the weight loss below 120 °C was ascribed to water evaporation for both β-CD and β-CDSP.[25] Then, a large mass loss peak occurred at about 310–350 °C because of the decomposition of cyclodextrin, and a final weight loss to 9.15% of the initial weight occurred for β-CD. The TGA curve of β-CDSP shows a multi-stage weight loss from 275 °C to 435 °C, where the decomposition temperature of β-CDSP was higher than that of β-CD. This may be due to the degradation of cyclodextrin and its functional groups. After 540 °C, a residual weight of 4.01% of the initial weight remained and decomposed slowly as a residue with high thermal stability. Such results indicated significant improvement in the thermal stability of β-CDSP after the polymerization of β-CD and styrene.

Adsorption of dyes

Influence of adsorption time. By plotting the adsorption capacities of NR, BF and ST dyes *versus* adsorption time at different concentrations (T = 25 °C, pH = 8), we report the corresponding results of adsorption (Fig. 3). It is clear that the adsorption increased promptly at the initial stages because of rapid attachment of the dyes to β-CDSP.[26] After 90 min, the adsorption showed no significant enhancement and became constant for BF and ST. Thus, the time of 90 min is sufficient for reaching the adsorption equilibrium for the two dyes. The adsorption of NR increased rapidly before 120 min and kept increasing gradually until the equilibrium was reached by prolonging the contact time. According to the adsorption curves, a much higher q_t value was presented for BF and ST than that for NR because of their different structures.

Adsorption kinetics. To further investigate the adsorption behavior of the three dyes on β-CDSP, commonly used pseudo-first order and pseudo-second order models were employed to describe the experimental results.[27] The pseudo-first order rate expression of Lagergren is given as the following equation:

$$q_t = q_e(1 - e^{-k_1 t}) \quad (1)$$

The pseudo-second order model proposed by Ho and McKay is represented in the following form:

$$q_t = \frac{k_2 q_e^2 t}{1 + k_2 q_e t} \quad (2)$$

Here, k_1 (min^{-1}) and k_2 (g mg^{-1} min^{-1}) are the rate constants of the pseudo-first order and pseudo-second order models, respectively, q_t (mg g^{-1}) and q_e (mg g^{-1}) are the adsorption capacities of the dye on β-CDSP at any time t and at equilibrium, and t (min) is the adsorption time.

By non-linear fitting the experimental data to the two models, we report the kinetic parameters of NR, BF and ST adsorbed onto β-CDSP (Table 1). It can be seen that both the pseudo-first order and the pseudo-second order rate expressions (R^2 > 0.99) have good agreement with the experimental data for NR and BF. The higher coefficients of the two models

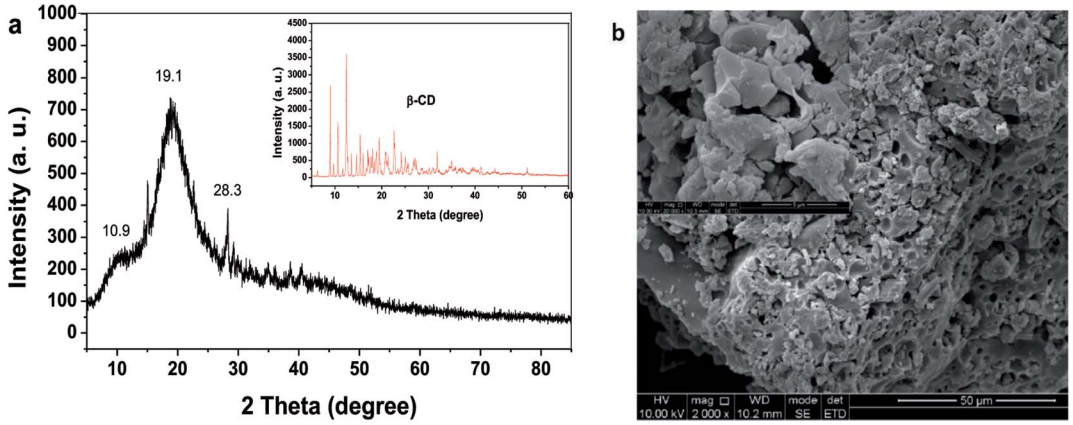

Fig. 2 (a) XRD pattern of β-CDSP (inset displays XRD pattern of β-CD); (b) SEM image of β-CDSP.

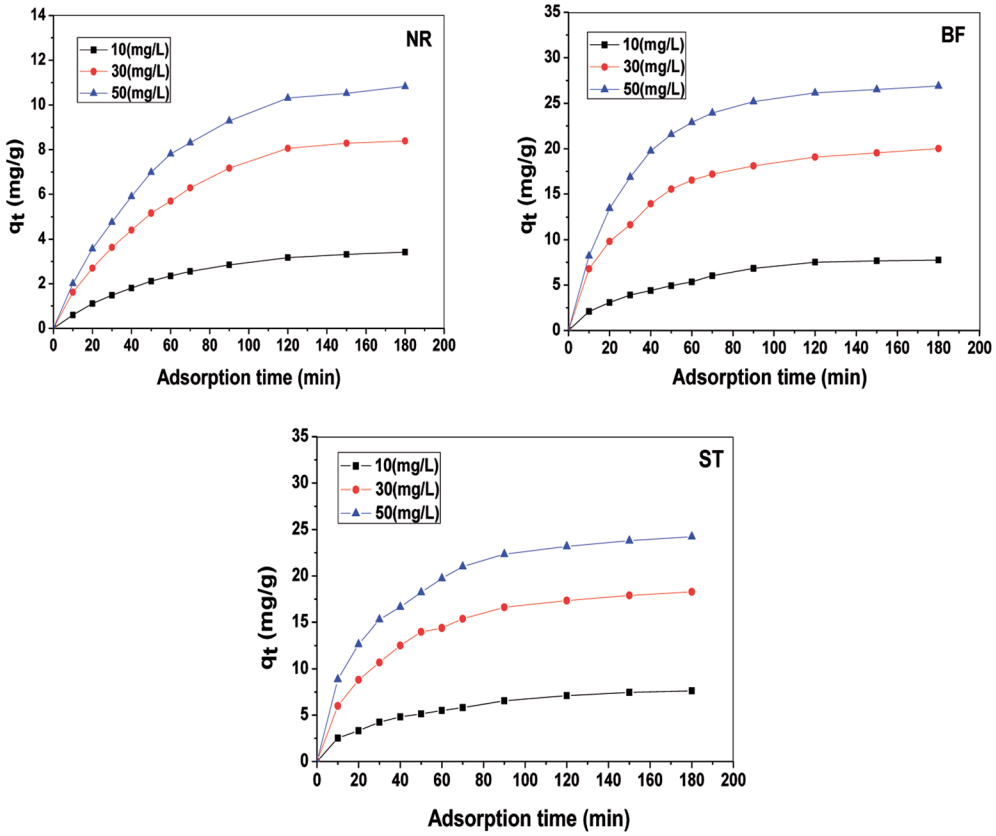

Fig. 3 Effect of adsorption time on NR, BF and ST dye adsorption capacity of β-CDSP under different initial concentrations.

suggested that the adsorption of the three dyes on β-CDSP was not only a chemisorption process but also a diffusion-controlled process.[28] However, the pseudo-second-order model fitted better than the pseudo-first-order model for ST. It seems that the greater number of chemical interactions generated from the cationic dyes and carboxyl groups on the adsorbent can account for this process. Moreover, with an increase of the solution concentration, the adsorption rate was found to be slow due to the occupied active sites on the surface of β-CDSP.

Influence of temperature. Temperature plays an important role in the adsorption process. Fig. 4 shows the adsorption results of NR, BF and ST on β-CDSP with initial dye concentrations of 5–100 mg L^{-1} at different temperatures (25, 35, 45, 55 and 65 °C) and pH = 8. Adsorption times of 90 min for BF and ST and 120 min for NR were selected. The results show that the adsorption capacity at equilibrium increased with the increase in temperature for all the three dyes. Especially for NR, the adsorbed amount was influenced greatly by temperature, and the largest divorce value of q_e was found to be 8.60 mg g^{-1} at 60 mg L^{-1} of dye concentration from 25 to 55 °C. The adsorbed amounts of BF and ST, in contrast, were less influenced by temperature and slightly increased with the increase in temperature. Moreover, the adsorption capacity tended to be steady and reached saturation after a rapid increase at low

Table 1 Kinetic parameters of NR, BF and ST dye adsorption on β-CDSP

Dye	Concentration (mg L^{-1})	q_e (exp) (mg g^{-1})	First-order kinetic model			Second-order kinetic model		
			k_1 (min^{-1})	q_e (cal) (mg g^{-1})	R^2	k_2 (g mg^{-1} min^{-1})	q_e (cal) (mg g^{-1})	R^2
NR	10	3.85	0.0181	3.5584	0.9998	0.0034	4.7247	0.9978
	30	8.66	0.0176	8.9207	0.9981	0.0013	11.9043	0.9951
	50	11.31	0.0191	11.2703	0.9991	0.0012	14.8385	0.9946
BF	10	6.75	0.0293	6.6299	0.9985	0.0041	8.0026	0.9945
	30	22.32	0.0292	22.2368	0.9933	0.0012	26.9520	0.9957
	50	29.56	0.0298	28.8886	0.9963	0.0009	34.9713	0.9913
ST	10	6.32	0.0397	6.1801	0.9910	0.0071	7.1602	0.9914
	30	21.69	0.0282	20.6703	0.9848	0.0013	24.9753	0.9952
	50	26.58	0.0299	25.7782	0.9863	0.0011	30.8998	0.9953

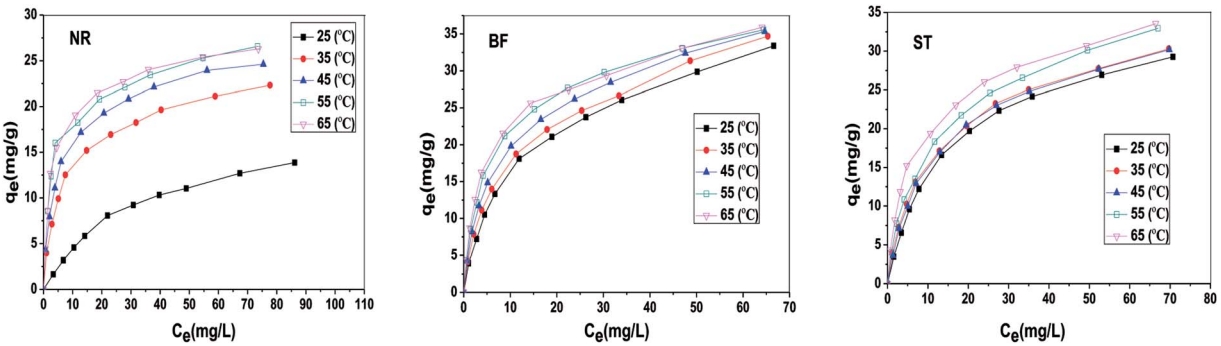

Fig. 4 Equilibrium adsorption of NR, BF and ST on β-CDSP at different temperatures.

initial concentrations (<60 mg L^{-1}). This is likely due to the occupation of active sites on β-CDSP. Thermodynamic parameters including the enthalpy change (ΔH^0), entropy change (ΔS^0) and Gibbs free energy change (ΔG^0) were utilized to describe the adsorption process of the three dyes on β-CDSP. These parameters were calculated by the following equations:[29,30]

$$\Delta G^0 = -RT \ln K_D \quad (3)$$

$$\ln K_D = \frac{\Delta S^0}{R} - \frac{\Delta H^0}{RT} \quad (4)$$

$$\lim_{C_e \to 0} \frac{q_e}{C_e} = K_D \quad (5)$$

Here, K_D is the equilibrium constant, which becomes dimensionless when the adsorbate solution is very dilute, R is the universal gas constant (8.314 J mol^{-1} K^{-1}) and T is the absolute temperature (K); ΔH^0 and ΔS^0 can be calculated by the slope and intercept of the plot of ln K_D *vs.* $1/T$.

The obtained thermodynamic parameters are listed in Table 2. The positive values of ΔH^0 revealed that the adsorption of NR, BF and ST dyes on β-CDSP was an endothermic process, which induced the increase of adsorption capacity with increasing temperature. The negative values of ΔG^0 suggested that the absorption process of the three dyes was spontaneous and favorable at all the studied temperatures. All the ΔS^0 values were positive, suggesting an increase in the randomness at the solid/solution interface during the adsorption,[31,32] which increased the contact opportunities between the dye molecules and β-CDSP and enhanced the adsorption. These results showed that the adsorption of NR, BF and ST dyes on β-CDSP was more favorable at a relatively higher temperature.

Adsorption isotherms. The widely used Langmuir and Freundlich isotherm models were utilized to analyze the experimental equilibrium data at a constant temperature in the present study. The linear equations are given as follows:[25,33]

$$\text{Langmuir}: q_e = \frac{q_m K_L C_e}{1 + K_L C_e} \quad (6)$$

$$\text{Freundlich}: q_e = K_F C_e^{1/n} \quad (7)$$

Here, C_e (mg L^{-1}) and q_e (mg g^{-1}) are the solution concentration and adsorption capacity of dye at equilibrium, respectively, K_L (L g^{-1}) is the Langmuir isotherm constant, q_m (mg g^{-1}) is the maximum adsorbed amount of dye, and K_F (L g^{-1}) and n are the Freundlich constant and the heterogeneity factor, respectively.

Table 3 shows the correlation coefficients (R^2) and isotherm parameters of the Langmuir and Freundlich isotherm models. The Langmuir adsorption model with larger values ($R^2 > 0.99$) provided a better fit than the Freundlich model for NR, BF and ST dye adsorption. This result confirmed that the adsorption process of the dyes on β-CDSP included the formation of a monolayer onto the homogenous adsorbent surface, and the adsorption occurred at specific sites of the adsorbent. The maximum adsorption capacities (q_m) of NR, BF and ST dyes on the adsorbent were determined to be 29.46, 63.64 and 49.01 mg g^{-1}, respectively. Better adsorption results were presented for BF dye due to higher affinity with β-CDSP.

Table 2 Thermodynamic parameters for NR, BF and ST dye adsorption on β-CDSP

Dye	NR			BF			ST		
Temperature (°C)	ΔG^0 (kJ mol^{-1})	ΔH^0 (kJ mol^{-1})	ΔS^0 (J/K mol)	ΔG^0 (kJ mol^{-1})	ΔH^0 (kJ mol^{-1})	ΔS^0 (J/K mol)	ΔG^0 (kJ mol^{-1})	ΔH^0 (kJ mol^{-1})	ΔS^0 (J/K mol)
25	−8.47	46.86	190.30	−10.97	21.19	107.24	−11.13	0.68	36.18
35	−13.20			−11.53			−11.81		
45	−14.36			−12.84			−13.36		
55	−15.85			−14.15			−11.70		
65	−16.40			−15.05			−12.92		

Table 3 Isotherm parameters of NR, BF and ST dye adsorption on β-CDSP

	Model	Langmuir			Freundlich		
Dye	Temperature (°C)	K_L (L g^{-1})	q_m (mg g^{-1})	R^2	K_F (L g^{-1})	n	R^2
NR	25	0.0305	18.38	0.9970	1.4495	1.9304	0.9796
	35	0.1734	27.26	0.9958	5.9685	3.1697	0.9756
	45	0.2283	29.46	0.9975	7.5221	3.4407	0.9721
	55	0.3343	28.84	0.9709	9.0678	3.8203	0.9556
	65	0.3426	28.09	0.9884	9.3710	3.8941	0.9525
BF	25	0.0838	53.32	0.9963	5.7023	2.3391	0.9887
	35	0.0903	63.64	0.9961	6.5092	2.4648	0.9918
	45	0.1285	52.27	0.9976	7.7056	2.6691	0.9967
	55	0.1793	43.80	0.9966	9.0631	2.9260	0.9740
	65	0.2116	43.86	0.9921	9.7391	3.0918	0.9739
ST	25	0.0893	39.13	0.9985	4.9254	2.3104	0.9747
	35	0.1008	49.01	0.9988	5.8044	2.4926	0.9826
	45	0.1565	45.18	0.9959	5.4975	2.4158	0.9782
	55	0.0730	36.65	0.9991	6.3250	2.4808	0.9867
	65	0.0994	41.53	0.9990	8.0606	2.8540	0.9810

Influence of solution pH. For dye adsorption, it is very important to study the pH values of the solution during the adsorption process. The acidity and basicity of the solution can easily change the surface charges of both the adsorbent and adsorbate and influence their properties.[27] Fig. 5 shows the effect of the initial solution pH on the adsorption of NR, BF and ST by β-CDSP. It is clear that the adsorption of BF and ST on β-CDSP increased sharply within the pH range measured in this study. Meanwhile, the results showed similar adsorption capacity for NR at pH < 8. It is reasonable that NR molecules enter the cavities of CD more easily compared to BF and ST with larger volume structures due to steric hindrance. Inclusion complexation makes major contribution towards NR adsorption. The faster enhancement of BF adsorption in a pH range from 2 to 8 is ascribed to stronger π–π interactions between the benzene rings on the adsorbent and BF molecule. With an increase in pH, the decreased protonation of the carboxyl groups on β-CDSP is favorable for decreasing the repulsive forces between the adsorbent and dyes.[34] The highest adsorption values can reach up to 8.775 mg g^{-1} for ST at pH = 12.

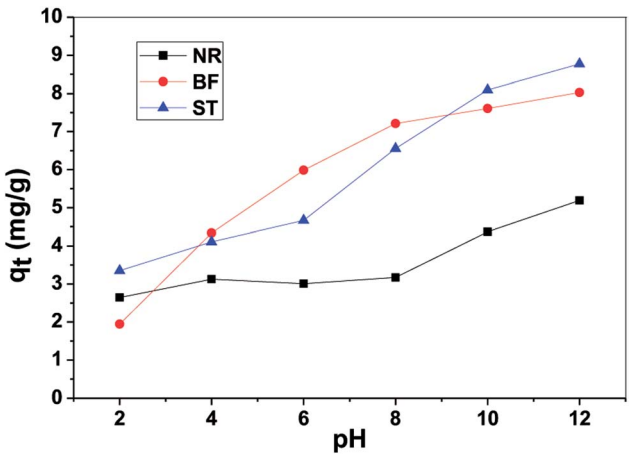

Fig. 5 Effect of pH on NR, BF and ST dye adsorption capacities of β-CDSP.

Mechanism of adsorption. According to the above results, a better adsorption capacity of β-CDSP was obtained for BF and ST than for NR. This can be due to the different chemical structures of the dyes and the change in charges of β-CDSP in different conditions. Compared with BF and ST, NR, with a line structure, easily enters the cavity of CD to form an inclusion complex. However, for BF and ST with more amino groups and a larger conjugation system, stronger electrostatic interactions with the carboxyl groups and π–π interactions with the benzene rings on β-CDSP were observed during the adsorption process. Especially for the adsorption in acidic solutions, the inclusion complexation and π–π interactions between β-CDSP and adsorbates contribute significantly to the adsorption of the three dyes. In addition, the carboxyl groups on the polymer are protonated under acidic conditions, which weakens the electrostatic interactions between β-CDSP and cationic dyes. With an increase in pH values, the increasing deprotonation of carboxyl groups makes the surface of the adsorbent process negatively charged and enhances the electrostatic interactions with amino groups on dyes. Thus, the adsorption capacity improved greatly for the three dyes, and a higher pH is more favorable for the adsorption of the three cationic dyes by β-CDSP. Besides inclusion complexation and π–π interactions, electrostatic interactions play an important role in this process in basic conditions. Scheme 2 presents the adsorption mechanism of NR, BF and ST on β-CDSP.

Recyclability of the adsorbent. It is important to estimate the stability and reusability of an adsorbent in view of its practical application. In this study, the adsorption performance of β-CDSP was evaluated for four sequential cycles of adsorption–desorption at the initial concentration of 10 mg L^{-1} and pH = 8. The adsorption temperature was maintained constant at 25 °C. The dye-loaded cyclodextrin polymer was regenerated after washing with solvent HCl (0.1 M), deionized water and ethanol.

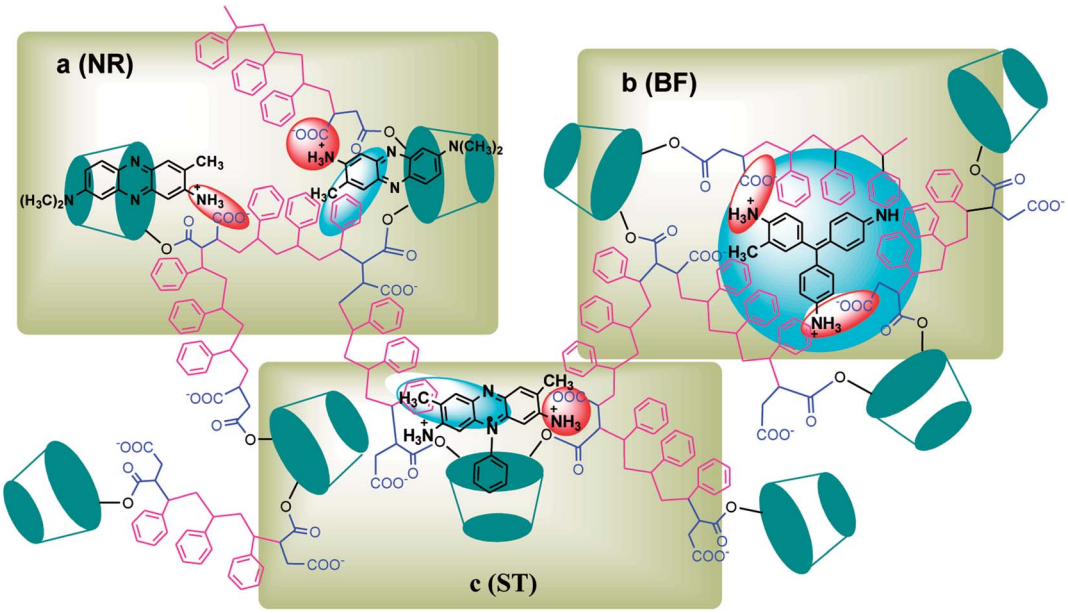

Scheme 2 Adsorption mechanisms of NR (a), BF (b) and ST (c) on β-CDSP.

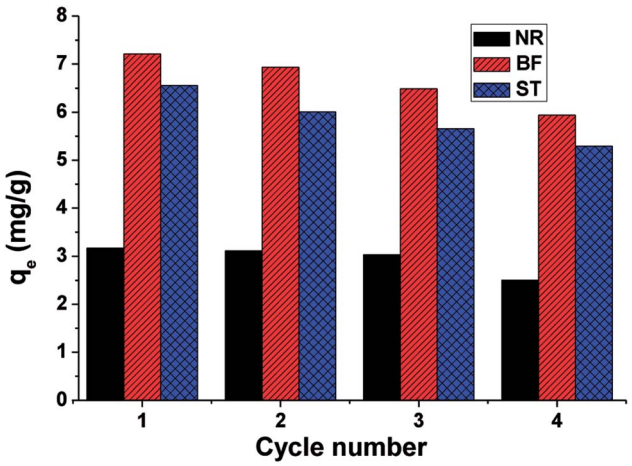

Fig. 6 The adsorption capacities of NR, BF and ST dyes on β-CDSP at different cycle numbers.

Fig. 6 shows the results of the recovery experiments. After four sequential cycles, the adsorption capacities of NR, BF and ST dyes on β-CDSP did not decrease significantly and the values were 78.86, 82.33 and 80.71% of the initial adsorption values, respectively. It is evident that β-CDSP as an excellent adsorbent is stable and reusable for adsorbing the three cationic dyes.

Conclusions

In this paper, β-CDSP with carboxyl groups and aromatic rings was developed and characterized as a new adsorbent for dyes. The adsorption capacities of NR, BF and ST dyes on β-CDSP were studied under different adsorption conditions such as adsorption times, temperatures and pH values. The experimental data showed that the adsorption equilibrium could be reached within 90 min for BF and ST and 120 min for NR. The adsorption kinetics data were fitted well with the pseudo-first order and the pseudo-second-order models for NR and BF and with the pseudo-second-order model for ST. The results suggested that both chemisorption process and diffusion-controlled process contributed to the adsorption of the three dyes on β-CDSP. A higher temperature was favorable for the adsorption of the three dyes by β-CDSP. The thermodynamic data revealed that the adsorption of NR, BF and ST dyes on β-CDSP was an endothermic and spontaneous process. The adsorption behavior was fitted to a Langmuir model, signifying monolayer adsorption. The results of pH studies illustrated that the adsorption capacities of the dyes on β-CDSP were enhanced greatly with increasing pH values. In a basic medium, the electrostatic interactions between the deprotonated carboxyl groups on β-CDSP and the amino groups on the dyes played an important role in the adsorption process. Moreover, inclusion complexion and π–π interactions were also dominant mechanisms of the three cationic dyes adsorbed by β-CDSP. After four regeneration cycles, the q_e values of the dyes on β-CDSP were still about 80% of the initial adsorption values. These results showed that β-CDSP is an effective adsorbent for adsorbing NR, BF and ST dyes.

Conflicts of interest

The authors declare no conflicts of interest.

Acknowledgements

This study was financial supported by the National Natural Science Foundation of China (No. 21605133 and 21602209), Shanxi Provincial Natural Science Foundation (No. 2014021015-

2 and 2013011040-5), and Post-doctoral Research Project of Hebei Province, China (B2016003028).

References

1 H. Bahria and Y. Erbil, *Dyes Pigm.*, 2016, **134**, 442–447.
2 S. Natarajan, H. C. Bajaj and R. J. Tayade, *J. Environ. Sci.*, 2018, **65**, 201–222.
3 L. Pérez-Ibarbia, T. Majdanski, S. Schubert, N. Windhab and U. S. Schubert, *Eur. J. Pharm. Sci.*, 2016, **93**, 264–273.
4 M. Ceborska, K. Kędra-Królik, A. A. Kowalska and M. Koźbiał, *Carbohydr. Polym.*, 2018, **184**, 47–56.
5 J. Kicuntod, W. Khuntawee, P. Wolschann, P. Pongsawasdi and T. Rungrotmongkol, *J. Mol. Graphics Modell.*, 2016, **63**, 91–98.
6 M. Ceborska, *J. Mol. Struct.*, 2018, **1165**, 62–70.
7 S. Li, L. Yuan, B. Zhang, W. Zhou, X. Wang and D. Bai, *RSC Adv.*, 2018, **8**, 25941–25948.
8 X. Li and Z. Zhou, *Anal. Chim. Acta*, 2014, **819**, 122–129.
9 J. Fiori, B. Pasquin, C. Caprini, S. Orlandini, S. Furlanett and R. Gotti, *J. Chromatogr. A*, 2018, **1562**, 115–122.
10 J. Y. Chen, S. R. Cao, C. X. Xi, Y. Chen, X. L. Li, L. Zhang, G. M. Wang, Y. L. Chen and Z. Q. Chen, *Food Chem.*, 2018, **239**, 911–919.
11 P. Tang, Q. Sun, Z. Suo, L. Zhao, H. Yang, X. Xiong, H. Pu, N. Gan and H. Li, *Chem. Eng. J.*, 2018, **344**, 514–523.
12 H. Liu, X. Cai, Y. Wang and J. Chen, *Water Res.*, 2011, **45**, 3499–3511.
13 G. Crini and H. N. Peindy, *Dyes Pigm.*, 2006, **70**, 204–211.
14 G. Crini, *Dyes Pigm.*, 2008, **77**, 415–426.
15 E. Yilmaz, S. Memon and M. Yilmaz, *J. Hazard. Mater.*, 2010, **174**, 592–597.
16 Y. Jiang, B. Liu, J. Xu, K. Pan, H. Hou, J. Hu and J. Yang, *Carbohydr. Polym.*, 2018, **182**, 106–114.
17 G. Z. Kyzas, N. K. Lazaridis and D. N. Bikiaris, *Carbohydr. Polym.*, 2013, **91**, 198–208.
18 T. Gong, Y. Zhou, L. Sun, W. Liang, J. Yang, S. Shuang and C. Dong, *RSC Adv.*, 2016, **6**, 80955–80963.
19 A. S. K. Kumar and S. J. Jiang, *J. Mol. Liq.*, 2017, **237**, 387–401.
20 A. P. Sherje, B. R. Dravyakar, D. Kadam and M. Jadhav, *Carbohydr. Polym.*, 2017, **173**, 37–49.
21 V. T. Fidal and T. S. Chandra, *Enzyme Microb. Technol.*, 2018, **116**, 57–63.
22 T. Umebayashi, Y. UtsumiI, S. Koga, S. Inoue, Y. Shiiba, K. Arakawa, J. Matsumura and K. Oda, *Tree Physiol.*, 2007, **27**, 993–999.
23 Y. Zhao, Y. Chen, J. Zhao, Z. Tong and S. Jin, *Sep. Purif. Technol.*, 2017, **188**, 329–340.
24 Z. Wang, P. Zhang, F. Hu, Y. Zhao and L. Zhu, *Carbohydr. Polym.*, 2017, **177**, 224–231.
25 Y. Z. Jiang, B. C. Liu, J. K. Xu, K. L. Pan, H. J. Hou, J. P. Hu and J. K. Yang, *Carbohydr. Polym.*, 2018, **182**, 106–114.
26 C. Srikantan, G. K. Suraishkumar and S. Srivastava, *Bioresour. Technol.*, 2018, **257**, 84–91.
27 Y. Zhou, Y. Hu, W. Huang, G. Cheng, C. Cui and J. Lu, *Chem. Eng. J.*, 2018, **341**, 47–57.
28 J. P. Simonin, *Chem. Eng. J.*, 2016, **300**, 254–263.
29 R. Elmoubarki, F. Z. Mahjoubi, H. Tounsadi, J. Moustadraf, M. Abdennouri, A. Zouhri, A. El Albani and N. Barka, *Water Resources and Industry*, 2015, **9**, 16–29.
30 T. S. Frantz, N. Silveira Jr1, M. S. Quadro, R. Andreazza, A. A. Barcelos, T. R. S. Cadaval Jr and L. A. A. Pinto, *Environ. Sci. Pollut. Res.*, 2017, **24**, 5908–5917.
31 H. Kono and T. Nakamura, *React. Funct. Polym.*, 2013, **73**, 1096–1102.
32 X. He, Z. Wu, Z. Sun, X. Wei, Z. Wu, X. Ge and G. Cravotto, *J. Mol. Liq.*, 2018, **255**, 160–167.
33 N. A. Salahuddin, H. A. EL-Daly, R. G. E. Sharkawy and B. T. Nasr, *Polymer*, 2018, **146**, 291–303.
34 L. Moulahcene, M. Skiba, O. Senhadji, N. Milon, M. Benamor and M. Lahiani-Skiba, *Chem. Eng. Res. Des.*, 2015, **97**, 145–158.